THE ASTRONOMICAL JOURNAL, 118:1347–1353, 1999 September

NEWLY DISCOVERED HERBIG-HARO OBJECTS IN THE NGC 2068 AND NGC 2071 REGIONS

BING ZHAO,[1,2,3] MIN WANG,[2,4] JI YANG,[2,4] HONGCHI WANG,[2,4] LICAI DENG,[1,2,3] JUN YAN,[2,4] AND JIANSHENG CHEN[1,2,3]
Received 1999 February 16; accepted 1999 May 19

ABSTRACT

Taking the advantage of the large field of view at the 60/90 cm Schmidt telescope of Beijing Astronomical Observatory, we were able to carry out a wide-field survey of Herbig-Haro (HH) objects in nearby star-forming regions, including Perseus, Taurus, Orion, and others. In a 58′ × 58′ field centered on NGC 2068 and NGC 2071 (M78), two active regions of star formation in the giant molecular cloud complex L1630, we found 17 HH objects exhibiting prominent [S II] emission but without continuum emission. Among these, we confirmed all the 11 known HH objects listed in the General Catalogue of Herbig-Haro Objects in this field. In addition, we discovered another six new HH objects, including HH 437, 438A–C, 440A/B, 442, 443, and 452A/B. These objects exhibit a variety of morphological structures, from knot to nebula. The discovery of these HH objects demonstrates strong activity of young stellar objects in the region we are studying. The large-scale spatial distribution of HH objects in the region is discussed by combination of our results and previous data.

Key words: ISM: Herbig-Haro objects — ISM: individual (NGC 2068, NGC 2071) — ISM: jets and outflows — stars: formation — stars: pre–main-sequence

1. INTRODUCTION

Herbig-Haro (HH) objects are shock-excited nebulae intimately associated with star-forming regions (Schwartz 1978). As one of the important processes of star formation (Reipurth & Heathcote 1997), HH objects, together with CO molecular outflows and shock-excited near-infrared emissions of H_2, are good tracers of the mass outflow activity of young stellar objects (YSOs) (see, e.g., Reipurth & Heathcote 1997). Up to now, more than 400 HH objects have been found via several search methods (Reipurth 1999).[5]

As part of a Galactic plane survey of HH objects, we observed a 58′ × 58′ field centered at M78 (NGC 2068, NGC 2071), located in the northern portion of L1630 (Orion B). The illuminating stars for the NGC 2068 reflection nebula are HDE 38563A and 38563B, while the illuminating star for NGC 2071 is HDE 290861. A large number of Hα emission stars (Haro & Moreno 1953; Herbig & Kuhi 1963) were found in this region. Eleven HH objects (HH 19–27, 37, and 70) have been discovered in this field (Herbig & Kuhi 1963; Herbig 1974; Strom et al. 1986; Reipurth & Graham 1988). Five CO outflows (HH 26 IR, HH 24, NGC 2068, NGC 2071, and NGC 2071N) were found in or near this region (White & Phillips 1981; Snell & Edwards 1982; Bally 1982; Fukui et al. 1986). An H_2O maser was discovered in the NGC 2071 region (Schwartz & Buhl 1975). As part of the L1630 cloud, the field we are studying has been surveyed using several different tracers of molecular gas, such as CO (Maddalena et al. 1986; Bally et al. 1991; Sakamoto et al. 1994), ^{13}CO (Bally et al. 1991; Sakamoto et al. 1994), and CS (Lada 1990; Lada, Bally, & Stark 1991a). A 2.2 μm (*K*-band) survey (Lada et al. 1991b), a 1.3 mm dust emission survey (Launhardt et al. 1996), and *IRAS*-based surveys for H_2O masers (Wouterloot & Walmsley 1986) and NH_3 emission (Wouterloot, Walmsley, & Henkel 1988) have also been conducted. In this work, we report the observation of HH objects toward the NGC 2068 and NGC 2071 regions.

2. OBSERVATIONS AND DATA REDUCTION

2.1. *Observations*

The observations were conducted with the 60/90 cm Schmidt telescope at Xinglong Observatory, Beijing Astronomical Observatory, Academia Sinica. A thick Ford 2048 × 2048 CCD having 15 μm pixels was mounted at the f/3 prime focus. The field of view of this CCD is 58′ × 58′, equivalent to 1.″71 pixel^{-1} (Chen 1994; Fan et al. 1996). Two BATC[6] intermediate-band filters, [BATC09] and [BATC10], together with a narrowband [S II] filter, were used by this program. Parameters of this set of filters are given in Table 1 (see also Yan et al. 1998). The [BATC09] filter covers well the strong and characteristic lines of HH objects ([N II], [Hα], [S II] λλ6717, 6731), while the [BATC10] band covers no line characteristic of HH objects (including the four lines mentioned above) and thus is used to measure the continuum emission. As explained in our previous work (Yan et al. 1998), three or more frames in the [BATC09], [BATC10], and [S II] bands are taken for a certain target field. This field in the region of M78 (including both NGC 2068 and NGC 2071) was observed during two runs. On 1996 March 14, we made the [BATC09] and [BATC10] observations. On 1997 March 10, we made the [S II] observations. Each image was processed through a series of programs termed PIPELINE-I (Fan et al. 1996; Zheng 1998). Dome flat-field normalization and other operations were done automatically by the programs. Each individual image was then inspected visually to check the quality. To this target field (NGC 2068 and NGC 2071), all the images were acceptable. As a

[1] Beijing Astronomical Observatory, Chinese Academy of Sciences, Zhongguancun, Beijing 100012, China.
[2] Chinese National Astronomical Observatories, Chinese Academy of Sciences, A20 Datun Road, Chaoyang District, Beijing 100012, China.
[3] Beijing Astrophysical Center, Academia Sinica, Peking University, Beijing 100871, China.
[4] Purple Mountain Observatory, Academia Sinica, 2 Beijing Xi Lu, Nanjing, Jiangsu 210008, China.
[5] See http://casa.colorado.edu/hhcat.
[6] The Beijing-Arizona-Taiwan-Connecticut Multicolor Sky Survey.

TABLE 1

PARAMETERS OF CCD IMAGING OF THE NGC 2068 AND NGC 2071 REGIONS

Filter	Central Wavelength (Å)	Bandwidth (Å)	Total Exposure Time (s)	Image Size (pixels)	Sky Level (ADU pixel^{-1})
[BATC09].....	6660	480	1200	2034 × 2046	1041.59
[BATC10].....	7050	300	1200	2034 × 2047	335.92
[S II]	6725	50	3600	2014 × 2046	221.03

result, all the images from the same filter were combined into a single frame and the position of the common center, derived using the Guide Star Catalog (GSC) of the Space Telescope Science Institute (Lasker et al. 1990), was put into the header of the combined image.

2.2. *Data Reduction*

After the PIPELINE-I reduction process and combination, we obtained the clean images from each filter, which are described in Table 1. As previously, our survey sequence includes two steps (Yan et al. 1998). (1) A quick survey for HH candidates: If an object is present in the combined [BATC09] image and absent in the combined [BATC10] image, it is regarded as a candidate HH object. Contamination by bright rims of H II regions and reflection nebulae is still possible after this step. (2) Narrowband identification: A deep exposure in [S II] was taken. The exposure time of each band we adopt makes the images of HH objects in the [S II] frames sharper than those in the [BATC09] frames. If a candidate object is present in the combined [S II] image, it is identified as an HH object. During the identification of each bona fide HH object, a careful examination of the morphology of the selected emission-line object is needed. In practice, further improvement to the above procedure was made so that those objects present in the [S II] image and absent in the [BATC10] image are identified as HH objects directly (after examination of the morphology). A set of IRAF-based programs was developed to search for HH objects semiautomatically (Zheng 1999). As a result, the HH-like point sources and extended sources can be picked up separately. Both the two-step procedure and the automatic programs for surveying the HH candidates were applied to the NGC 2068/NGC 2071 field in this work.

3. RESULTS AND DISCUSSION

In this survey, 17 HH objects with prominent [S II] emission are identified in the NGC 2068 and NGC 2071 regions; the overall locations of the 17 HH objects in NGC 2068 and NGC 2071 are illustrated in Figure 1. We found that among the 17 HH objects, we have confirmed all the 11 known HH objects of the region listed by Reipurth (1999), including HH 19–27, 37, and 70. Besides these known HH objects, we have found six new HH objects. They are HH 437, 438A–C, 440A/B, 442, 443, and 452A/B. In Table 2, we list the coordinates of the six newly discovered HH objects. Using the Guide Star Catalog, we obtained an astrometric accuracy comparable to the GSC system (Fan et al. 1996).

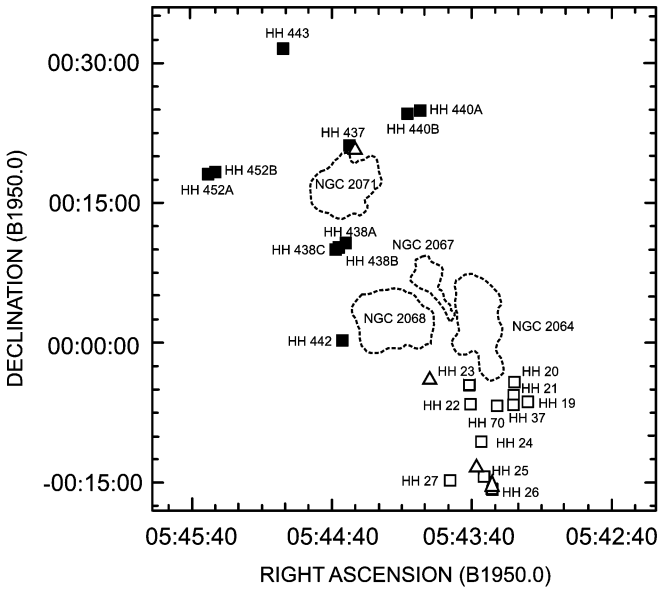

FIG. 1.—Schematic representation of the locations of HH objects in the NGC 2068 and NGC 2071 regions. The newly discovered HH objects are marked with filled rectangles. The known HH objects are marked with open rectangles and the known outflows with open triangles, which, from north to south, are NGC 2071, NGC 2068, HH 24, and HH 26 IR. The dashed lines outline the reflection nebulae.

TABLE 2

NEW HERBIG-HARO OBJECTS IN THE NGC 2068 AND NGC 2071 REGIONS

Object	α (B1950.0)	δ (B1950.0)	Angular Size (arcsec)	Linear Size (pc)	Position Angle (deg)	Comments
HH 440A.....	05 44 02.10	00 25 00.0	36	0.082	20	Bright nebula with a tail
HH 440B.....	05 44 08.06	00 24 36.1	7	0.016	...	Knot
HH 437.....	05 44 31.54	00 20 47.6	16	0.037	...	Knot with fuzzy nebula
HH 438A.....	05 44 33.48	00 10 45.2	21	0.048	30	Nebula with a bright core
HH 442.....	05 44 35.40	00 00 15.2	12	0.027	...	Knot
HH 438B.....	05 44 37.01	00 10 05.2	31	0.071	30	Nebula
HH 438C.....	05 44 38.16	00 10 02.7	16	0.037	140	Nebula
HH 443.....	05 45 01.16	00 31 36.0	16	0.037	...	Knot with a tail
HH 452B.....	05 45 30.32	00 18 17.3	23	0.053	...	Irregular nebula
HH 452A.....	05 45 33.15	00 17 59.6	19	0.043	...	Fuzzy nebula

NOTE.—Units of right ascension are hours, minutes, and seconds, and units of declination are degrees, arcminutes, and arcseconds.

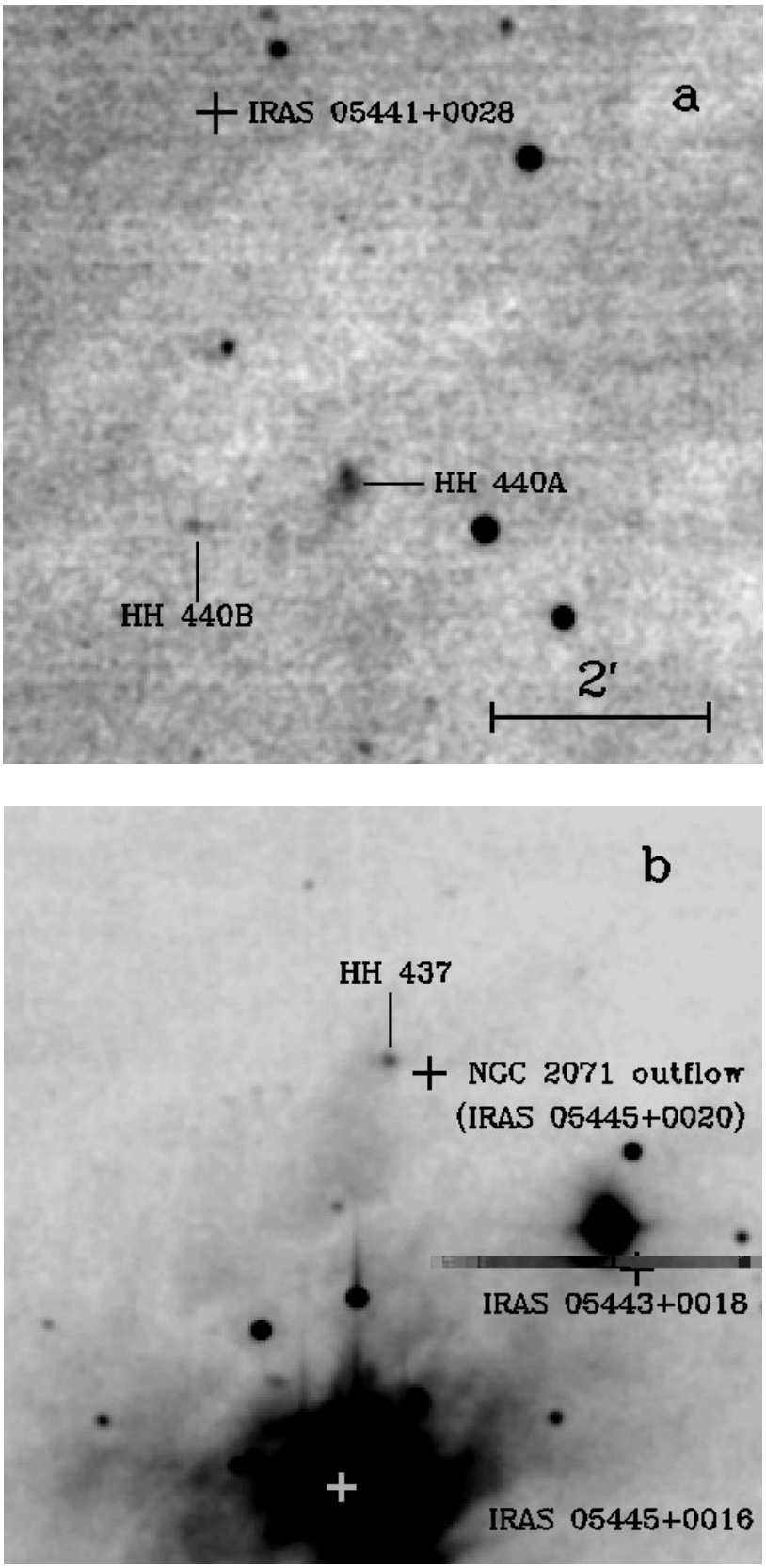

FIG. 2.—[S II] images of the newly discovered HH objects: (*a*) HH 440, (*b*) HH 437, (*c*) HH 438, (*d*) HH 442, (*e*) HH 443, (*f*) HH 452. The two white plus signs in (*f*) are stars. All the fields are 7′ × 7′; north is up, east is to the left, and the scale is shown in (*a*).

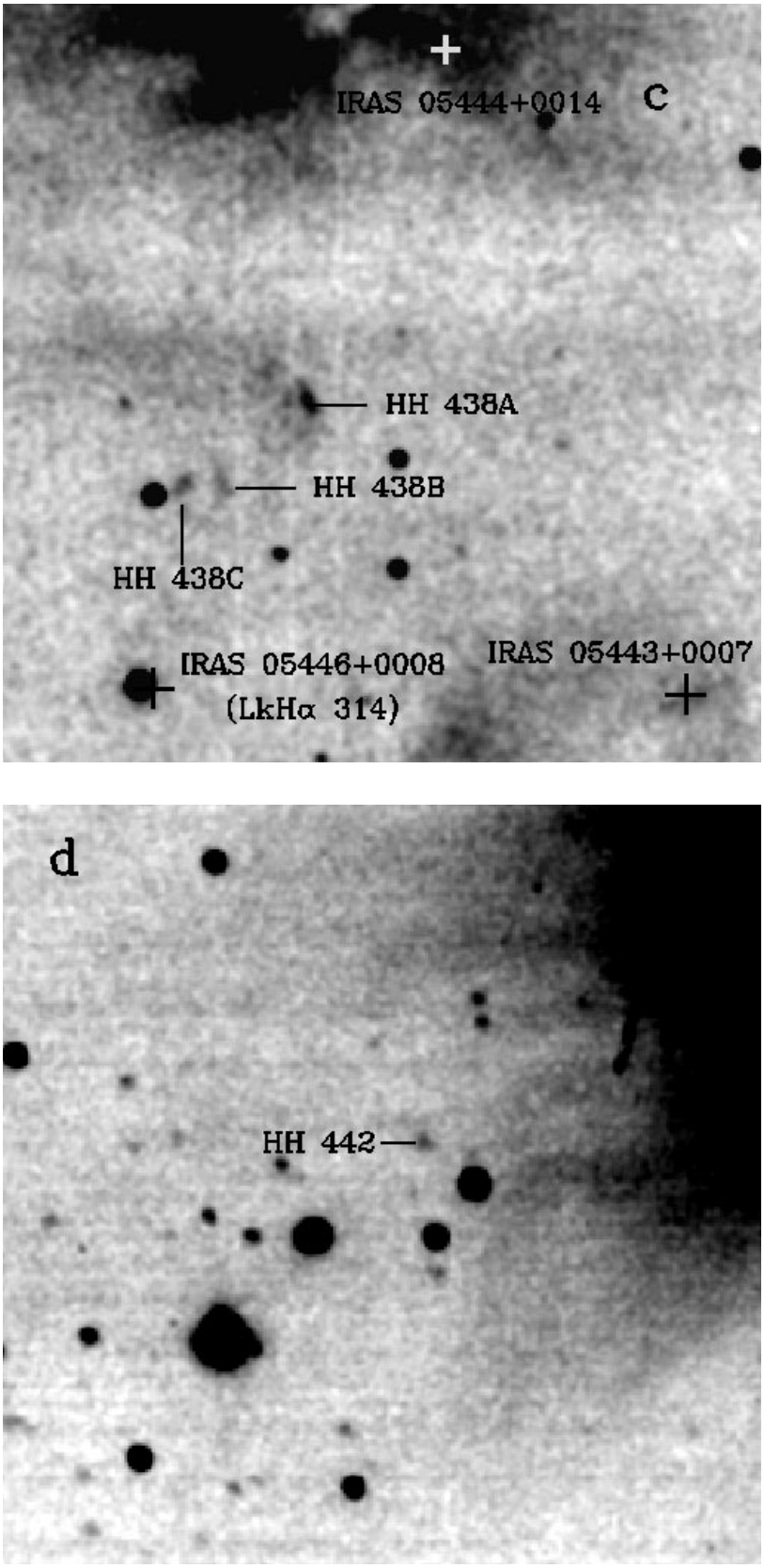

FIG. 2.—*Continued*

All these objects (including the known ones and the newly discovered ones) fall into two enhanced regions, one in the southwest region of NGC 2064 and NGC 2068, and another in the NGC 2071 region (Fig. 1).

HH 440A/B (Fig. 2*a*) are in the northwest part of NGC 2071. HH 440A is a bright nebula with a tail protrusion toward the southeast. Along the line toward the reverse direction of this tail, we find a star about 3.′28 (0.45 pc)

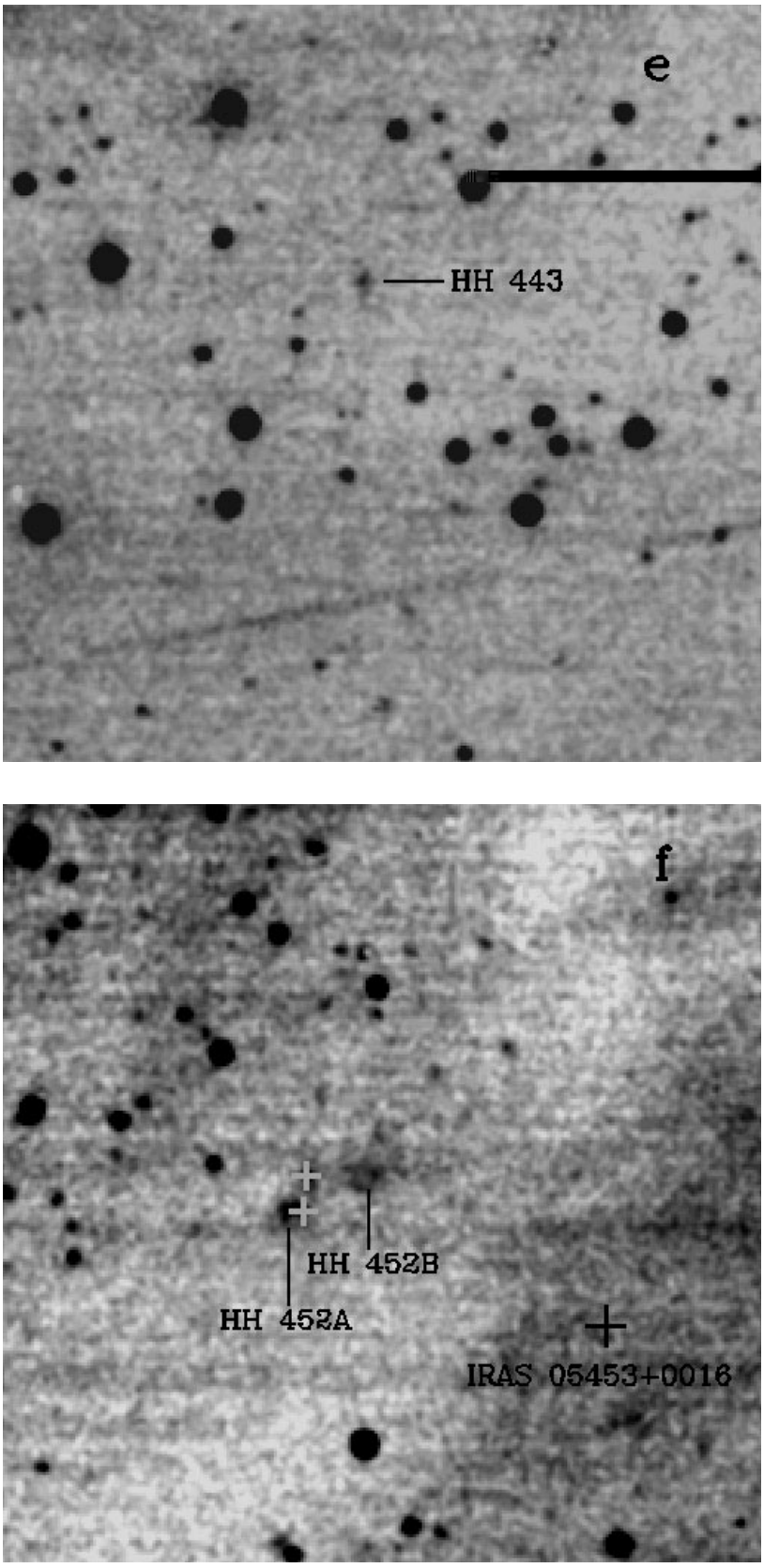

FIG. 2.—*Continued*

northwest of HH 440A. Based on the locations of HH 440A and the bright star and the orientation of the tail, we suppose that the star is responsible for the tail. HH 440B is a knot with an angular size of about 7″ (0.016 pc). IRAS 05441+0028 is about 3.′7 north of HH 440A/B. The stellar object lying between the *IRAS* source and HH 440 is not an HH object, because it is also present in the [BATC10] image. Another faint knot is visible between HH 440B and

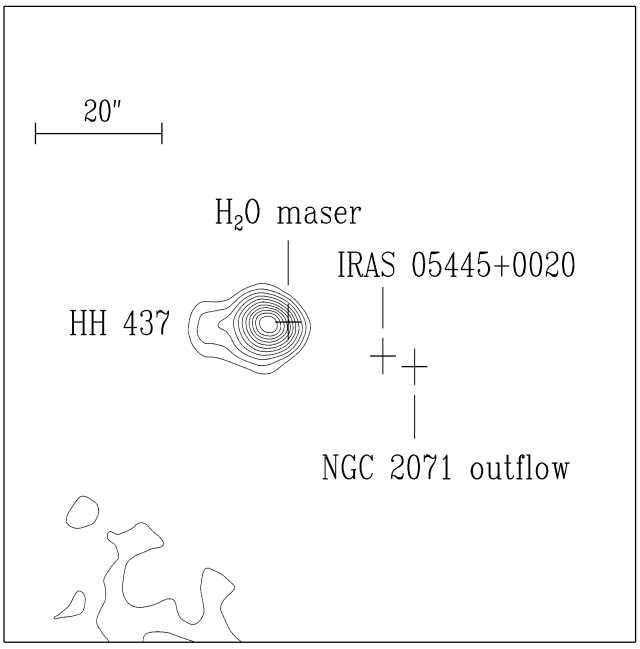

FIG. 3.—Contour plot of HH 437. The field is 1.′7 × 1.′7. The lowest contour level is 5 times the rms noise; the contour step is 2 times the rms noise. In order to compress the noise, a circular Gaussian function was adopted to convolve the image. The σ of the Gaussian function is 1 pixel (1.″71).

the tail of HH 440A. The morphology of HH 440A/B and the knot suggests another possibility, that the three objects may constitute a bow shock driven by IRAS 05441+0028. Observation with higher spatial resolution and deeper exposure should help to identify more details and the interrelation among these objects.

HH 437 (Fig. 2*b*) is a bright knot with a fuzzy nebula to the north of NGC 2071. From the contour plot (Fig. 3) and our [S II] image, we can find a short tail toward the east. HH 437 is close to the center of the well-known bipolar

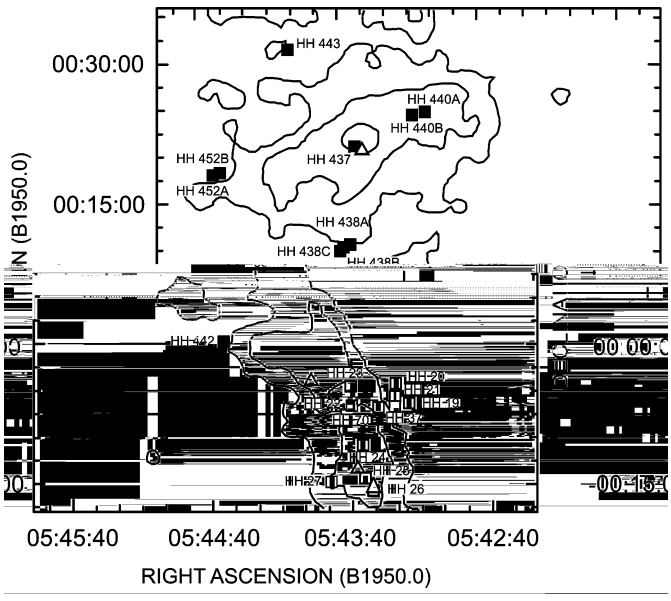

FIG. 4.—Schematic representation of the locations of HH objects in the NGC 2068 and NGC 2071 regions. The contours of the CS $J = 2$–1 line emission are taken from Lada (1992).

molecular outflow NGC 2071 (Bally 1982; Fig. 2*b*). The redshifted lobe of the outflow is in P.A. = 225° (Snell et al. 1984). IRAS 05445+0020 (NGC 2071 IRS 1, GL 818), one of the youngest YSOs and candidate protostars (Wynn-Williams 1982; Fukui et al. 1993; Pollanen & Feldman 1995), is believed to be the exciting source of the CO outflow (Bally 1982; Berrilli et al. 1989). In addition, HH 437 coincides with an H_2O maser (Schwartz & Buhl 1975; Genzel & Downes 1979) within the positional error (Fig. 3). The relative positions of HH 437, the H_2O maser, and the NGC 2071 outflow (IRAS 05445+0020) are illustrated by the contour plot in Figure 3. Considering the proximity of these objects, we have much confidence that HH 437, the NGC 2071 outflow, and the H_2O maser contribute to the same outflow origin. Also, from the morphology of HH 437 and the relative position of HH 437 with respect to the blueshifted and redshifted lobes of the molecular outflow, we speculate that HH 437 is part of the blueshifted outflow.

HH 438A–C (Fig. 2*c*) are located between NGC 2068 and NGC 2071. HH 438A is an irregular nebula with a bright core, while HH 438B/C are two relatively weak nebulae. All of them are elongated. HH 438A/B have approximately the same position angle (30°) and are 1.′06 (0.15 pc) away. In the nearby region, three *IRAS* sources, IRAS 05443+0007, 05444+0014, and 05446+0008 (LkHα 314), can be found. Among them, IRAS 05446+0008 (LkHα 314) is a classical T Tauri star (Herbig & Bell 1988; Weintraub 1990). Though none of the three *IRAS* sources align with the patches of HH 438, we cannot exclude the possibility that the *IRAS* sources, especially IRAS 05446+0008 (LkHα 314), are the exciting source of HH 438A–C.

HH 442 (Fig. 2*d*) is a knot located at the east periphery of the NGC 2068 nebula. Neither an *IRAS* source nor another YSO indicator is found near it, and its exciting source is not clear from the available data.

HH 443 (Fig. 2*e*) is an isolated HH knot on the far north side of NGC 2071. It shows a tail toward the south. Since no *IRAS* source is found near the object, we believe the knot-tail structure is driven by an unknown YSO source somewhere along the direction opposite to the tail.

HH 452A (Fig. 2*f*) is a fuzzy nebula connecting with a star. HH 452B is an irregular nebula with an angular size of 23″ (0.053 pc). Both HH 452A and 452B are to the east of NGC 2071. In the nearby region, IRAS 05453+0016 is about 3.′23 (0.44 pc) and 2.′75 (0.38 pc) southwest of HH 452A and 452B, respectively. This source shows rising fluxes at 60/100 μm (*IRAS* Point Source Catalog 1985), suggesting a YSO nature. At present, the *IRAS* source can be identified as the most possible exciting source of the two nebulae.

The 17 HH objects identified in this survey follow the general trend of the dense molecular gas, as illustrated by their projection onto the CS map in Figure 4. They are not uniformly distributed throughout the surveyed field. Most fall roughly into two enhanced regions, except HH 442. One enhanced region is in the southern part of the NGC 2068 CS dense molecular gas (Fig. 4), obviously separated from the bright NGC 2068 reflection nebula. HH objects in this region include all of the known ones (HH 19–27, 37, and 70) and appear highly grouped or clustered. We estimate the surface number density of this area to be $\sim$410 deg^{-2}. Three molecular outflows (NGC 2068, HH 24, and HH 26 IR) are located within or close to this enhanced region. The relative concentration of HH objects and molecular outflows indicates active star formation in this region.

The other enhanced region coincides with the dense CS gas in NGC 2071 (Fig. 4). Different from the clustered HH objects of NGC 2068, the HH objects in this region (HH 437, 438, 440, 443, and 452) are rather uniformly distributed. However, the surface number density is only ~ 40 deg^{-2}, 1 order of magnitude lower than that of the NGC 2068 region. HH objects in this region are distributed along the peripheral area of the NGC 2071 reflection nebula, in contrast to the first group of HH objects, which are isolated away from the bright nebula NGC 2068. These differences in spatial distribution of HH objects may imply different physical environments and star formation processes in the two enhanced regions.

The 2.2 μm survey by Lada et al. (1991b) revealed two embedded infrared clusters in NGC 2068 and NGC 2071. The two IR clusters are spatially coincident with the NGC 2068 and NGC 2071 optical nebulae, as demonstrated by contour maps of surface density of infrared sources (see Figs. 5, 6*c*, and 6*d* in Lada et al. 1991b) and Figure 4. Comparison with the location of these IR clusters shows that the HH objects have quite different spatial distributions. Most (16 out of 17) are located beyond the enhanced peak of infrared sources, except HH 437. This kind of spatial separation may reflect different epoch of star formation or the consequence of formation of stars of different mass.

4. CONCLUSION

1. Six new HH objects have been discovered in our survey, including HH 437, 438A–C, 440A/B, 442, 443, and 452A/B. Moreover, we confirm all the 11 already known HH objects in this field.

2. HH 437 coincides with an H_2O maser within the positional error and lies close to the center of the NGC 2071 outflow.

3. All the HH objects follow the general trend of the dense molecular gas and roughly fall into two enhanced regions. One region is in the southern part of NGC 2068, with a surface number density of ~ 410 deg^{-2}. The other coincides with the dense CS gas in NGC 2071, with a surface number density of ~ 40 deg^{-2}.

4. HH objects in the first enhanced region are separated from the NGC 2068 nebula, as well as the infrared cluster. HH objects in the second region are distributed along the peripheral area of the NGC 2071 nebula, as well as the IR cluster.

We acknowledge the staff members of the BATC Beijing group for excellent support during observations and Z. Y. Zheng for developing the software. We are very grateful to Y. Wu and S. Luo for helpful discussions. We appreciate Bo Reipurth for assigning the HH numbers and also for his valuable comments on our objects. This research was supported by grants from the Natural Science Foundation of China.

REFERENCES

Bally, J. 1982, ApJ, 261, 558
Bally, J., Langer, W. D., Wilson, R. W., Stark, A. A., & Pound, M. W. 1991, in IAU Symp. 147, Fragmentation of Molecular Clouds and Star Formation, ed. E. Falgarone, F. Boulanger, & G. Duvert (Dordrecht: Kluwer), 11
Berrilli, F., Ceccarelli, C., Liseau, R., Lorenzetti, D., Saraceno, P., & Spinoglio, L. 1989, MNRAS, 237, 1
Chen, J. 1994, in IAU Symp. 161, Astronomy from Wide-Field Imaging, ed. H. T. MacGillivray, E. B. Thomson, B. M. Lasker, I. N. Reid, D. F. Malin, R. M. West, R. M., & H. Lorenz (Dordrecht: Kluwer), 17
Fan, X., et al. 1996, AJ, 112, 628
Fukui, Y., Iwata, T., Mizuno, A., Bally, J., & Lane, A. P. 1993, in Protostars and Planets III, ed. E. H. Levy & J. I. Lunine (Tucson: Univ. Arizona Press), 603
Fukui, Y., Sugitani, K., Takaba, H., Iwata, T., Mizuno, A., Ogawa, H., & Kawabata, K. 1986, ApJ, 311, L85
Genzel, R., & Downes, D. 1979, A&A, 72, 234
Haro, G., & Moreno, A. 1953, Bol. Obs. Tonantzintla Tacubaya, No. 7, 11
Herbig, G. H. 1974, Lick Obs. Bull., No. 658
Herbig, G. H., & Bell, K. R. 1988, Lick Obs. Bull., No. 1111
Herbig, G. H., & Kuhi, L. V. 1963, ApJ, 137, 398
IRAS Point Source Catalog. 1985, Joint *IRAS* Science Working Group (Washington: GPO)
Lada, E. A. 1990, Ph.D. thesis, Univ. Texas, Austin
———. 1992, ApJ, 393, L25
Lada, E. A., Bally, J., & Stark, A. A. 1991a, ApJ, 368, 432
Lada, E. A., DePoy, D., Evans, N. J., & Gatley, I. 1991b, ApJ, 371, 171
Lasker, B. M., Sturch, C. R., McLean, B. J., Russell, J. L., Jenkner, H., & Shara, M. M. 1990, AJ, 99, 2019
Launhardt, R., Mezger, P. G., Haslam, C. G. T., Kreysa, E., Lemke, R., Sievers, A., & Zylka, R. 1996, A&A, 312, 569
Maddalena, R. J., Morris, M., Moscowitz, J., & Thaddeus, P. 1986, ApJ, 303, 375
Pollanen, M., & Feldman, P. A. 1995, PASP, 107, 617
Reipurth, B. 1999, General Catalogue of Herbig-Haro Objects (2d ed.; Boulder: Cent. Astrophys. Space Astron.)
Reipurth, B., & Graham, J. A. 1988, A&A, 202, 219
Reipurth, B., & Heathcote, S. 1997, in IAU Symp. 182, Herbig-Haro Flows and the Birth of Low Mass Stars, ed. B. Reipurth & C. Bertout (Dordrecht: Kluwer), 3
Sakamoto, S., Hayashi, M., Hasegawa, T., Handa, T., & Oka, T. 1994, ApJ, 425, 641
Schwartz, P. R., & Buhl, D. 1975, ApJ, 201, L27
Schwartz, R. D. 1978, ApJ, 223, 884
Snell, R. L., & Edwards, S. 1982, ApJ, 259, 668
Snell, R. L., Scoville, N. Z., Sanders, D. B., & Erickson, N. R. 1984, ApJ, 284, 176
Strom, K. M., Strom, S. E., Wolff, S. C., Morgan, J., & Wenz, M. 1986, ApJS, 62, 39
Weintraub, D. 1990, ApJS, 74, 575
White, G. J., & Phillips, J. P. 1981, MNRAS, 194, 947
Wouterloot, J. G. A., & Walmsley, C. M. 1986, A&A, 168, 237
Wouterloot, J. G. A., Walmsley, C. M., & Henkel, C. 1988, A&A, 203, 367
Wynn-Williams, C. G. 1982, ARA&A, 20, 587
Yan, J., Wang, H., Wang, M., Deng, L., Yang, J., & Chen, J. 1998, AJ, 116, 2438
Zheng, Z. Y. 1998, Ph.D. thesis, Beijing Astron. Obs.
———. 1999, in preparation